Phys. Status Solidi A **207**, No. 4, 801–806 (2010) / **DOI** 10.1002/pssa.200983302

physica status solidi a
www.pss-a.com
applications and materials science

Theoretical simulation and preparation of binary and ternary combinatorial libraries by thermal PVD

Sebastian Oliver Klemm[1], Alistair Graeme Martin[1,2], Julia Lengsfeld[1], Janine-Christina Schauer[3], Bernd Schuhmacher[3], and Achim Walter Hassel[*,1,4]

[1] Max-Planck-Institut für Eisenforschung GmbH, Max-Planck-Str. 1, 40237 Düsseldorf, Germany
[2] School of Chemistry, The University of Edinburgh, Edinburgh, EH9 3JJ Scotland, UK
[3] Dortmunder OberflächenCentrum, Eberhardstr. 12, 44145 Dortmund, Germany
[4] Institute for Chemical Technology of Inorganic Materials, Johannes Kepler University, Altenberger Str. 69, 40404 Linz, Austria

Received 13 August 2009, revised 9 December 2009, accepted 11 December 2009
Published online 29 March 2010

Keywords binary metal alloys, ternary metal alloys, PVD, alloy surface, simulation

* Corresponding author: e-mail hassel@elchem.de, Phone: +43 732 2468 8704, Fax: +43 732 2468 8905

Binary and ternary composition spread material libraries were prepared using a thermal physical vapor deposition system with three separated heating sources and adjustable chamber geometry. In this work, we present binary Cu84-20Al16-80 and Zn71-8Mg29-92 libraries as well as a ternary Cu67-6Ag81-13Mg66-12 system with a thickness around 300 nm. The composition of the obtained films was determined by automated energy dispersive X-ray spectroscopy and the data further used to develop a mathematical model to simulate the surface. The thickness of a copper film was measured by atomic force microscopy and used to verify the theoretical model, whereas topography scans provided information on the surface roughness. The consistency between theoretical simulations and observed compositions concludes multiple source thermal co-evaporation to be a reliable method with high variety regarding source metals and deposition rates and therefore of high value for material library fabrication.

1 Introduction The combinatorial approach to develop new materials is a modern methodology [1–3]. It utilizes the capability to produce material libraries with a known dependence between location and composition in combination with high throughput investigation methods with high spatial resolution.

In general, the idea to use co-deposition techniques to vary the composition on the substrate dates back several decades and has been used to investigate ternary phase diagrams or superconductors [4, 5]. Advances in high throughput screening methods, in general the bottle neck of this approach, have further increased the potential for time efficient R&D [6].

Methods to fabricate combinatorial thin films include sputter deposition [7, 8], pulsed laser deposition [9], electron beam deposition [10], and thermal PVD [11].

The advantage of the latter can be seen in its flexibility both in deposition rate and film thickness, even though it is limited to metals with a sufficiently high vapor pressure.

Regarding zinc, aluminium, and magnesium as the most important metals for cathodic corrosion protection [12–14], all components are suitable for evaporation by thermal PVD.

It is therefore not surprising that various recent research activities are focussed on the issue to coat steel with Zn-alloys from the gas phase [15, 16]. Furthermore, combinatorial screening on binary or ternary material libraries provides valuable information selecting the most promising compositions for these coatings. A reliable fabrication and precise characterization of the film composition is crucial for this investigation.

The large number of metals suitable for thermal PVD allows the combinatorial investigation of alloy systems largely investigated by classical sample preparation. Copper–aluminum [17], copper–silver [18], and iron–zinc [19] are just a few examples with an electrochemical focus.

Advances in screening methods like small-spot XRD and local resistance measurements [20], small spot UV–Vis [21], and localized electrochemistry [22, 23] demand a high

accuracy relating composition and position on combinatorial libraries. To achieve high resolutions, the change in composition per length unit is desired to be sufficiently low to prevent the method itself to cover a significant composition spread. Therefore, the sample size is large compared to the spot subject to screening.

With respect to the accuracy of detection by quick and non-destructive analytical methods like EDX and XRF, typically higher for heavier metals, a mathematical model is a promising way to describe the composition over large surfaces with high tolerance against deviations in single spots caused, for example, by local contaminations or surface defects.

Additionally, surface-functions provide a way to determine the local composition of infinitely small spots on the library while not increasing the number of measurement points originally used to calculate the function.

The aim of this work is to introduce a thermal PVD system capable of producing binary and ternary material libraries from a variety of metals. Furthermore, the gradients obtained are analyzed from a mathematical perspective and a way to model and predict material libraries is presented.

2 Experimental

2.1 Thermal PVD The thermal PVD-system used in these studies contains a bell jar deposition chamber evacuated by a liquid-nitrogen baffled diffusion-pump with a rotary-vane fore-vacuum. The base pressure is approximately 2×10^{-4} Pa and rises to around 4×10^{-4} Pa during deposition. Three tungsten baskets (B12A 3x.030W, Testbourne Ltd., Basingstoke, UK) for thermal evaporation are powered by two 900 W DC- and one 1800 W AC-power supply.

To evaporate zinc, one basket was replaced by a tungsten coil with boron-nitride crucible (B8A 3x.025W and C1-BN, Testbourne Ltd., Basingstoke, UK) due to the high need for constant and gentle heating given the high vapor pressure of zinc.

Each source is located 80 mm above the base plate with a spacing of 110 mm with respect to the neighboring sources. Within this triangle, the substrate is placed 120–300 mm above the base plate, yielding aspect ratios between spacing and substrate height above the source from 2.75 to 0.37 (Fig. 1).

Deposition rates were constantly measured using Quartz Microbalances (QMBs) for each specific source well shielded from the others.

The tooling factors for the QMB were determined by placing a fourth QMB centered and about 60 mm above the sources, using the quotient of the central QMB and the sources QMB as a factor for further measurements.

Steady deposition rates were achieved by using a Labview based program, reading the QMB through a SQM-242 Interface card (Sigma Instruments, Fort Collins, USA) and controlling the power output of the power supplies utilizing a proportional-integral-regulation.

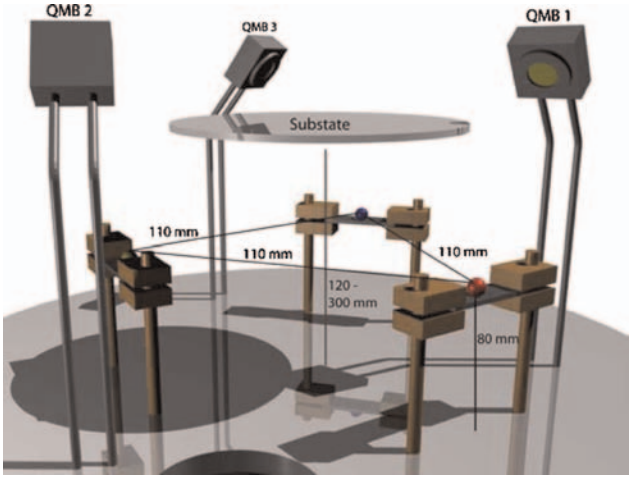

Figure 1 (online color at: www.pss-a.com) Schematic illustration of the PVD geometry.

Metals used for evaporation were obtained from Alfa Aeser (Alfa Aeser GmbH & Co KG, Karlsruhe, Germany) of at least 99.995% purity.

One hundred millimeter p-type Silicon Wafers (Si-Mat Silicon Materials, Landsberg am Lech, Germany) with a thickness of 525 ± 25 μm were taken as substrates from a sealed box without further cleaning.

2.2 EDX-element analysis A Zeiss LEO 1550 VP scanning electron microscope was used for automated composition mapping. A substrate characteristic like the wafer-flat or two fine marks are used to define an absolute point and a vector defining the x-plane. Depending on the geometry of the substrate, linear, rectangular, and matrices approximating a circle can be addressed automatically.

The results shown are always derived from spectra recorded with 10 kV acceleration voltage integrating 40 s. The penetration depth depends on the film composition and ranges from several hundred nanometers to a few micrometers. In every case, the substrate, if present, is substracted from the spectrum. Calibration is performed with cobalt and manganese (99.99%, Goodfellow, Huntingdon, England) on a 2-week schedule.

2.3 AFM Atomic force microscopic (AFM) topography scans were performed on a JPK NanoWizard I AFM (JPK Instruments AG, Berlin, Germany) operating in contact mode with a silicon cantilever (CONTR obtained from BudgetSensors, typical tip radius <10 nm).

The film thickness was measured by cutting the film at points spaced 10 mm along a line pointing away from the source using a surgical blade, thereby removing the film down to the blank substrate. A linear fit along the substrate-baseline and the film yields a z-shift directly correlating to the thickness as shown in Fig. 2.

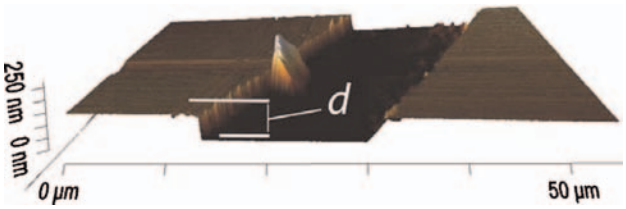

Figure 2 (online color at: www.pss-a.com) AFM 3D topography image over a cut showing the thickness d.

3 Results and discussion

3.1 Single source evaporation A pure copper-film was evaporated onto a $20 \times 90\ mm^2$ silicon substrate using a rate of $0.4\ nm\ s^{-1}$ and the long side pointing towards the source. AFM images were measured at 10 and 70 mm and the following topographies were obtained (Fig. 3).

Table 1 summarizes the roughness at both positions. The data does not reveal a dependence of the topography on the thickness or deposition rate, respectively. Both surfaces can be considered very smooth and appear perfectly reflective by optical inspection. The topography observed is comparable to previously published copper thin films prepared by cathodic vacuum arc technique [24].

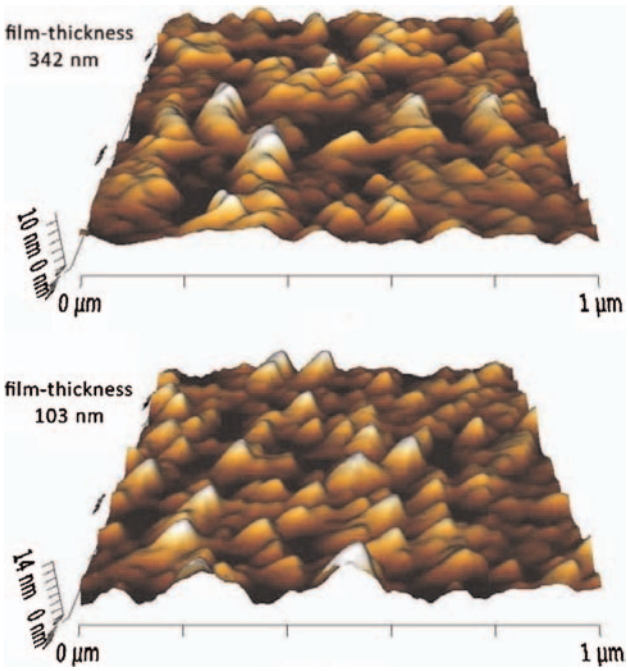

Figure 3 (online color at: www.pss-a.com) 3D AFM images ($1 \times 1\ \mu m^2$, Z-range 10 and 14 nm) of the copper film at different spots.

Table 1 Roughness information on pure copper with different thickness.

thickness (nm)	average roughness (nm)	root mean square roughness (nm)	peak to valley (nm)
342	1.3	1.7	6.3
103	1.4	1.8	6.6

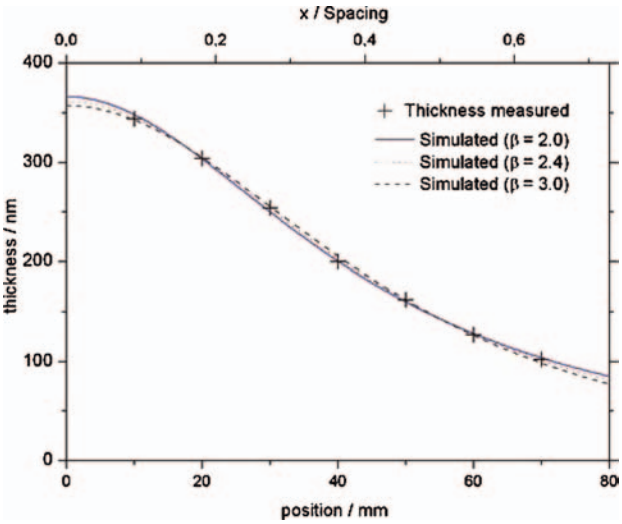

Figure 4 (online color at: www.pss-a.com) Measured film thickness of pure copper from a single evaporation source.

The thickness measured by AFM ranges from 342 down to 103 nm measured in 10 mm steps from the side located above the source. Figure 4 shows the thickness in relation to both, the absolute position on the substrate and the ratio between the x-position and the spacing between the sources.

The sigmoidal dependence between position and thickness can be described using a cosine depended model (Fig. 5).

Given a point source, a plane in the distance h being the substrate and a point above the source being x_0,y_0, the deposition-rate $R_{x,y}$ at a particular point is antiproportional to r^2 because a constant mass flow per angle covers a greater area with increasing θ. With R_{x_0,y_0} being the deposition rate above the source, the cosine model gives

$$R_\theta \approx R_{x_0,y_0} \cos^2(\theta) \tag{1}$$

and therefore

$$R_{x,y} = \frac{R_{x_0,y_0} h^2}{(x - x_0)^2 + (y - y_0)^2 + h^2}. \tag{2}$$

Besides this, desorption of species from flat sources has been discussed in literature and found to be angle dependent with respect to the surface normal [25–28].

Thus, breaking the assumption of an isotropic emission from a point source, the preferential direction of emission and geometric factors affect the rate found on the substrate. The deviation from the surface normal was described being depended on $\cos(\theta)$, giving

$$R_\theta = R_{x_0,y_0} \cos^\beta(\theta), \tag{3}$$

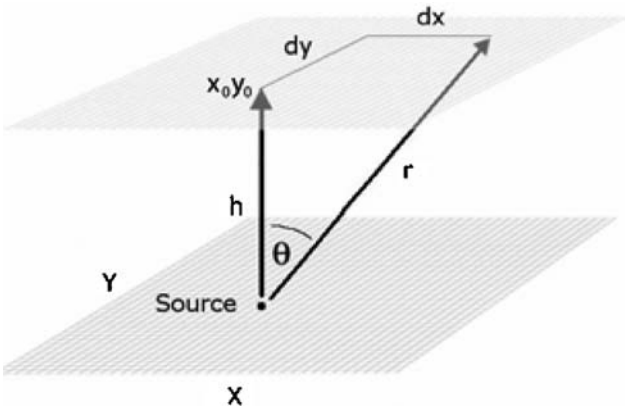

Figure 5 Schematic illustration of the geometric parameters.

with $\beta = 3.0$ for a point source with the preferential direction pointing towards x_0,y_0 according to the cosine desorption model.

The reason for β taking different values for different sources can be suspected in many effects.

The sources body may emit atoms in a preferential direction not following the cosine rule. This exponent was described as the sharpness parameter for the angular distribution of repulsive desorption [29].

Furthermore, depositions at acute angles cause an equal impact angle of the atoms on the surface. The sticking parameter, being the fraction of atoms adsorbed after hitting the surface, depends on the atoms energy, the surface properties [30], and the ability to transfer kinetic energy into the surface. The latter was reported to be cosine-shaped [31].

Finally, some source parameters like the temperature distribution within the glowing coil and the exact geometric shape are not known. Nevertheless, the present data suggests that a variation in the exponent of cosine provides an accurate and feasible way to average the numerous angle dependent influences.

A variation of the sharpness parameter and the theoretical height h, used to calculate the fitting curves in Fig. 4, are shown in Table 2. Additionally, the root mean square deviation (RMSD) is calculated.

With a measured height of 55 ± 5 mm, a sharpness parameter of 2.4 gives the best description of the real thickness.

Due to the high conformity demonstrated in Fig. 4, the thickness function regarding the x-position derived from Eqs. (2) and (3) for the copper film can be described as:

$$d_x = \frac{R_{x_0} h^{2.4} t}{((x - x_0)^2 + h^2)^{1.2}} \tag{4}$$

with d_x being the thickness at the corresponding x-position on the substrate, t being the time in seconds, and R_{x_0} being the deposition rate at x_0 in nanometres per second.

This relationship can be further used to perform thickness related measurements [32] on a large number of coordinates using the combinatorial approach.

Table 2 Model fit parameters used in Fig. 4.

β	h (mm)	RMSD
2.0	44	2.47
2.4	51	1.41
3.0	60	2.67

3.2 Dual source evaporation Aluminum and copper were co-evaporated using a rate of 0.2 nm s^{-1} for 800 s. Using the rates R_{Al} and R_{Cu} for the different sources, the number of moles emitted from a source A hitting a 1 cm^2 surface per second can be calculated using the density and molar mass according to the following equation:

$$N_A = \frac{\rho_A R_A}{10^7 M_A}. \tag{5}$$

This conversion is required to calculate the atomic ratio between aluminum and copper on each position on the substrate. The factor 10^7 reflects the conversion of nanometer to centimeter. The density ρ in formula 5 always needs to have the same value as the density used by the QMB for the specific source.

Additionally, the substrates rectangular shape demands the use of both, x and y coordinates to map and simulate the composition. Using the sharpness parameter from Eq. (3) and x_0 and y_0 as the position closest to source A, Eq. (2) translates into:

$$N_{A,x,y} = \frac{\rho_A R_A h^\beta}{10^7 M_A ((x - x_0)^2 + (y - y_0)^2 + h^2)^{\beta/2}}. \tag{6}$$

Plotting the quotient of N_{Al} and N_{Cu} in percent against the xy-coordinates, a three-dimensional (3D) surface graph was obtained as shown in Fig. 6. Given equal rates, the difference in density and molar mass determines a slight shift towards higher copper contents, yielding a Cu84Al16 to Cu20Al80 library.

The yellow spheres interconnected by lines represent a model fit using $R_{Cu}/R_{Al} = 1$, $h = 55$ mm, and $\beta = 2.4$. The points represent calculated compositions at the locations used for EDX-measurement with a diameter of 2 at.%. Therefore, a satisfactory match between the simulation and the measured surface displays yellow spheres partly visible through the surface. In this particular case, the RMSD was found to be 0.839 which gives an excellent mathematical description of the surface.

The Zn71Mg29–Zn8Mg92 gradient shown in Fig. 7 was produced by using $R_{Zn}/R_{Mg} = 1/3$ and fitted with $h = 55$, $\beta_{Zn} = 2.4$, and $\beta_{Mg} = 2.6$ giving a RMSD of 1.014.

These results show the opportunity to predict binary gradients prior to deposition and later derive the mathematical relationship between molar fraction and position. The need to maintain a large set of local composition scans in order to either address the previously characterized spots or calculate the local composition from neighboring data points

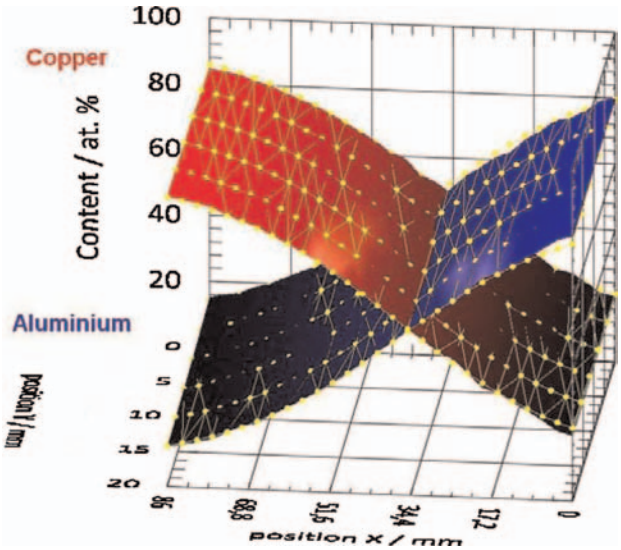

Figure 6 (online color at: www.pss-a.com) A binary Cu–Al gradient (colored surface plot) with model fit (yellow spheres/lines, see text).

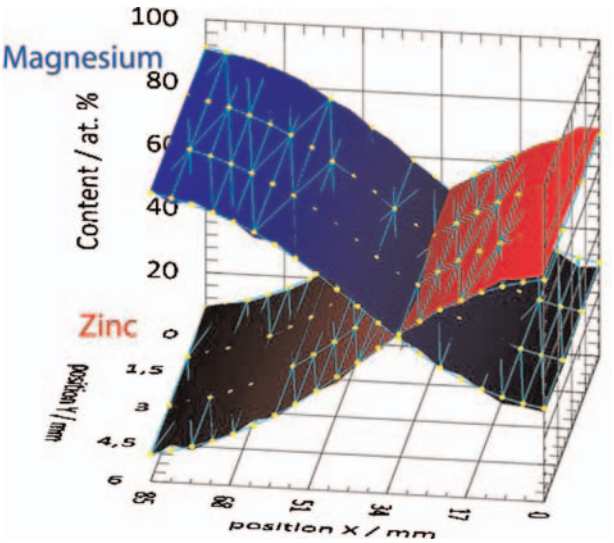

Figure 7 (online color at: www.pss-a.com) A binary Zn–Mg gradient with model fit.

is replaced by a single formula. Furthermore, a comparably small set of points can be used to generate surfaces covering large areas in relation to the spatial resolution of the following investigation.

It needs to be pointed out that the evaporation rates must be well controlled during the deposition process in order to avoid depth profiles showing deviations in concentration. Gradients subject to significant fluctuations in deposition rates will deviate from the sigmoid shape since the measured molar fraction will be the sum of all cosine functions over the penetration depth of the spectroscopic method.

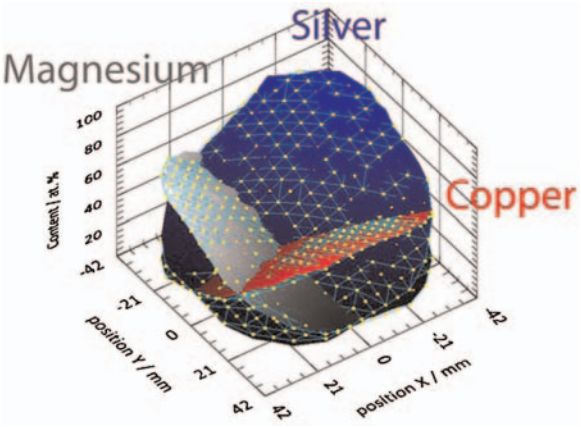

Figure 8 (online color at: www.pss-a.com) A Cu–Ag–Mg ternary library with model fit.

Table 3 Parameters and RMSD for a ternary Cu–Ag–Mg fit.

source	relative rate	h (mm)	β	RMSD
Cu	1.00	55	2.4	1.97
Ag	2.11	55	2.8	1.95
Mg	2.53	55	2.6	1.59

3.3 Triple source evaporation Copper, silver, and magnesium were evaporated on 100 mm silicon wafer using the following rates:

$$R_{Cu} = 0.2\,\mathrm{nm\,s^{-1}}$$
$$R_{Ag} = 0.4\,\mathrm{nm\,s^{-1}}$$
$$R_{Mg} = 0.4\,\mathrm{nm\,s^{-1}}$$

Figure 8 shows the 3D plot obtained by EDX and the simulated surfaces describing the gradient.

The parameters used to model the surfaces are shown in Table 3.

The model fit shown in Fig. 8 describes the surface with RMSDs less than 2%. It is obvious that the rates used for calculating the surface deviate from the rates measured during deposition. This reflects an inaccurate correction factor between the rate measured by the monitor balance and the rate observed on the substrate, called tooling factor. Deviations from the calibration occur due to changes in geometry and possibly different deposition rates of the metal on the quartz and the substrate.

The deposition rate can therefore be most accurately determined by a model fit of the surface which is another feature of the mathematical simulation.

4 Conclusions Binary and ternary material libraries of metals suitable for thermal PVD can be obtained by thermal co-deposition from refractory metal boats, baskets, or crucibles using a chamber-geometry described in this work.

The films show a smooth surface thus enabling accurate thickness-determination by AFM topography scans.

Both, the EDX-mapping and the thickness of the films can be simulated using a cosine-desorption approach described in this work. Furthermore, the mathematical description of the measured composition provides a way to navigate on the surface and relating the position to a composition with high and constant accuracy.

Due to variable chamber geometry and a suitable mathematical model, the mean content and the slope of its gradient can be predicted for each individual metal within the library. Therefore, high numbers of alloys of a variety of metals can be produced on a single substrate with a high potential for combinatorial material development.

Acknowledgements We acknowledge the financial and scientific support from Dortmunder OberflächenCentrum, Dortmund, Germany. A. G. Martin is indebted to the Deutscher Akademischer Austauschdienst for a fellowship within the frame of the RISE program.

References

[1] B. J. Chisholm and D. C. Webster, J. Coat. Technol. Res. **4**, 1 (2007).
[2] R. A. Dunlap, G. L. Sibley, F. N. Sy, and T. D. Hatchard, J. Alloys Compd. **470**, 27 (2007).
[3] H. Koinuma, H. N. Aiyer, and Y. Matsumoto, Sci. Technol. Adv. Mater. **1**, 1 (2000).
[4] K. Kennedy, T. Stefansky, G. Davy, V. F. Zackay, and E. R. Parker, J. Appl. Phys. **36**, 3808 (1965).
[5] J. J. Hanack, J. Mater. Sci. **5**, 964 (1970).
[6] I. Hashim, M. Mathur, P. Phatak, R. Kuse, S. Malhota, S. Barstow, S. Shanker, and T. Chiang, Solid State Technol. **52**, 26 (2009).
[7] R. Löbel, S. Thienhaus, A. Savan, and A. Ludwig, Mater. Sci. Eng. A **481**, 151 (2008).
[8] J. R. Dahn, S. Trussler, T. D. Hatchard, A. Bonakdarpour, J. R. Mueller-Nauhaus, K. C. Hewitt, and M. Fleischhauer, Chem. Mater. **14**, 3519 (2002).
[9] D. Craciun, G. Socol, N. Stefan, M. Miroiu, I. N. Mihailescu, A.-C. Galca, and V. Craciun, Appl. Surf. Sci. **255**, 5288 (2009).
[10] G. Garcia, R. Domenech-Ferrer, F. Pi, J. Santiso, and J. Rodriguez-Viejo, J. Comb. Chem. **9**, 230 (2007).
[11] A. I. Mardare, A. P. Yadav, A. D. Wieck, M. Stratmann, and A. W. Hassel, Sci. Technol. Adv. Mater. **9**, 035009 (2008).
[12] R. Hausbrand, M. Stratmann, and M. Rohwerder, J. Electrochem. Soc. **7**, C369 (2008).
[13] M. C. Quevedo and J. Genesca, Mater. Corr. **6**, 424 (2008).
[14] A. R. Marder, Prog. Mater. Sci. **45**, 191 (2000).
[15] I. A. Gorlach, Thin Solid Films **517**, 5270 (2009).
[16] B. Schuhmacher, C. Schwerdt, U. Seyfert, and O. Zimmer, Surf. Coat. Technol. **163**, 703 (2003).
[17] E. A. Ashour and B. G. Ateya, Electrochim. Acta **42**, 243 (1997).
[18] S. M. Skogvold, Q. Mikkelsen, G. Billon, C. Garnier, L. Lesven, and S.-F. Barthe, Anal. Bioanal. Chem. **384**, 1567 (2006).
[19] A. Besseyrias, F. Dalard, J. J. Rameau, and H. Baudin, Corr. Sci. **39**, 1883 (1997).
[20] R. Zarnetta, A. Savan, S. Thienhaus, and A. Ludwig, Appl. Surf. Sci. **254**, 743 (2007).
[21] J. Noh, Y. D. Suh, Y. K. Parl, S. M. Jin, S. H. Kim, and S. I. Woo, Rev. Sci. Instrum. **78**, 072205 (2007).
[22] A. W. Hassel and M. M. Lohrengel, Electrochim. Acta **42**, 3327 (1997).
[23] A. I. Mardare, A. Ludwig, A. Savan, A. D. Wieck, and A. W. Hassel, Electrochim. Acta **54**, 5171 (2009).
[24] J. R. Shi, S. P. Lau, Z. Sun, X. Shi, B. K. Tay, and H. S. Tan, Surf. Coat. Technol. **138**, 250 (2001).
[25] J. Noh, Y. D. Suh, Y. K. Park, S. M. Jin, S. H. Kim, and S. I. Woo, Rev. Sci. Instrum. **78**, 072205 (2007).
[26] M. Knudsen, Ann. Phys. Leipzig **353**, 1113 (1916).
[27] M. Knudsen, Ann. Phys. Leipzig **357**, 105 (1917).
[28] K. Stella, D. Bürstel, S. Franzka, O. Posth, and D. Diesing, J. Phys. D, Appl. Phys. **42**, 135417 (2009).
[29] T. Matsushima, Prog. Surf. Sci. **82**, 77 (2007).
[30] X.-Y. Liu, M. S. Daw, J. D. Kress, D. E. Hanson, V. Arunachalam, D. G. Coronell, C.-L. Liu, and A. F. Voter, Thin Solid Films **422**, 141 (2002).
[31] D. E. Hanson, J. D. Kress, and A. F. Voter, Phys. Rev. B **60**, 11723 (1999).
[32] Z. H. Cao, P. Y. Li, H. M. Lu, Y. L. Huang, and X. K. Meng, J. Phys. D **42**, 065405 (2009).

